DYNAMIC MODELING OF THROMBOELASTOGRAPHY TO INFORM STATE OF COAGULOPATHY IN TRAUMA PATIENTS

Michelle A. Pressly*[1], Matthew D. Neal[2,3], Gilles Clermont[1,2] and Robert S. Parker[1,2]

[1]Department of Chemical and Petroleum Engineering, University of Pittsburgh, Pittsburgh, PA 15260
[2]Department of Critical Care Medicine, University of Pittsburgh, Pittsburgh, PA 15260
[3]Department of Surgery, University of Pittsburgh, Pittsburgh, PA 15260

December 2nd, 2016

Abstract

Modeling clotting dynamics that occur during a thromboelastogram (TEG), a functional ex-vivo assay of coagulation, has the potential to provide useful clinical insights. Taking a systems view, the *ex vivo* system (TEG) dynamics are modeled without explicitly representing the complex *in vivo* clotting cascade. The model utilizes reaction engineering principles represented as ordinary differential equations (ODEs), which are solved in MATLAB (©2016, The Mathworks Inc.) or Python. The model structure uses linear kinetics, except for the thrombus growth rate, which has a quadratic dependence on activated platelets. Estimated parameters include the initial platelet count, platelet activation rate, thrombus growth rate, and lysis rate (P_0, k_1, k_2, and k_3, respectively). Parameter estimation via nonlinear least-squares optimization of model predictions against clinical data used PYOMO 4.3 with the IPOPT solver. For 60 sample TEG tracings, the model yielded an average relative error of 6.42%, which demonstrates a simple mathematical description of coagulation is able to capture TEG data. Multi-parameter distributions demonstrates patient variability, suggesting it may be possible to identify patient endotypes from these distributions. A model-informed endotyping of patient-specific coagulopathic state could guide clinicians in selecting individualized treatment decisions leading to improved patient outcomes.

Keywords

Nonlinear dynamic modeling, coagulation, thromboelastography, endotyping, biomedicine

Introduction

An impairment of the coagulation process (coagulopathy), especially in the acute response to trauma, increases the relative risk of death by 4.6 times in severely injured patients (Maegele et al., 2011). Furthermore, surviving patients with early onset coagulopathy more frequently develop multiple organ failure(Maegele et al., 2007). The variability associated with hemostasis, the process of stopping blood loss, is important for understanding the many biological phenotypes (observable traits) and their underlying endotypes (mechanisms) that lead to these severe clinical differences. These endotypes may prove important for informing medical decisions including determining which state of coagulopathy a patient is experiencing and what kind of treatment to administer after trauma (Liou et al., 2014). Thus, modeling coagulation of blood at an appropriate resolution could provide individual endotyping from phenotypic data, and ultimately improve clinical outcomes.

One assay for analyzing the state and functionality of blood hemostasis is the thromboelastogram (TEG), which analyzes a 340 μL sample of blood mixed with clotting factors. The device stand oscillates, simulating sluggish blood flow and naturally driving thrombus formation (clotting), which is measured by the displacement of a torsion pin (Hae, 2007). This assay can inform patient coagulopathic state quickly after entry into the

*To whom all correspondence should be addressed *map312@pitt.edu*

clinic. The key processes in the clotting cascade observed during a TEG are platelet activation, thrombus (clot) growth, and lysis of the clot. Modeling of the device response, and also the biological processes, can be accomplished at a variety of scales based on the physical and biochemical interactions of the components in blood (plasma, blood cells, platelets, clotting factors, etc.) that are activated during the assay. Currently the dynamics of this complex, multi-scale biological system are not entirely understood.

The clotting cascade has been modeled at a variety of scales (Xu et al., 2010; Bannish, 2014). Drawing upon the work of Jones and Mann (1994), complex high-order models of the extrinsic and extrinsic pathways including the various factors and physiological particles and molecules have been constructed (Xu et al., 2010; Anand et al., 2008; Lo et al., 2005). The application of such a model to individual patient TEG response is complicated by the number of available parameters and the inability to easily and uniquely map them individually to the impact they have on a TEG tracing. In contrast, a lumped model may not capture the full biological complexity of the system, but may still provide clinically-useful information about individuals through its ability to capture measurements and differentiate between patients and patient-populations. This can be approached on parametric grounds or through competing model structures. Such is the focus of this work, where a low-order model of TEG response is constructed and used to capture individual patient data from clinical trials.

Model Structure

The TEG response model was developed from the following simplified reaction scheme under the assumption that all reactions are irreversible. Conceptually, platelet activation (1) is followed by thrombus formation (2), which is ultimately broken down through the process of lysis (3).

$$P \rightarrow P_a \quad (1)$$

$$P_a \rightarrow T \quad (2)$$

$$T \rightarrow L \quad (3)$$

This reaction scheme is easily converted to the ordinary differential equation (ODE) representation (4)-(7), by treating the TEG device as a batch reactor. The states include free platelets, $P(t)$, activated platelets, $P_a(t)$, thrombus state, $T(t)$, and lysed thrombus, $L(t)$. The final state, while not a measurable molecule, *per se*, provides an integrated measure of total lysis, and thereby the lysis rate.

$$\frac{dP(t)}{dt} = -k_1 P(t) \quad (4)$$

$$\frac{dP_a(t)}{dt} = k_1 P(t) - k_2 P_a(t)^2 \quad (5)$$

$$\frac{dT(t)}{dt} = k_2 P_a(t)^2 - k_3 T(t) \quad (6)$$

$$\frac{dL(t)}{dt} = k_3 T(t) \quad (7)$$

Estimated parameters include the initial platelet number $P(0)$, platelet activation rate (k_1), thrombus growth rate (k_2), and lysis rate (k_3). The objective function was sum of squared error between clinical patient data and the thrombus state $T(t)$.

Before optimization, direct simulation was implemented in MATLAB (©2016, The MathWorks, Natick, MA) using the *ode15s* solver. Parameter ranges were set prior to optimization by using the SIMBIOLOGY package in MATLAB. This pharmacokinetic/pharmacodynamic modeling package allows for direct integration of model Eqs. (4)-(7) from the reaction scheme in Eqs. (1)-(3). Simbiology allows for parameter sweeps over orders of magnitude, with an easy interface to view the effect of these parameter values on the clinically-measurable thrombus state. Initial guesses for parameter estimation as well as the ranges determined for each parameter, are shown in Table 1.

Table 1. Initial guesses and search ranges for model parameters as determined from MATLAB's SIMBIOLOGY parameter sweeps. Note that the thrombus state must have units of mm to relate back to the TEG.

Parameter	Initial Guess	Range	Units
P_0	max(data)	0 - 70	Scalar
k_1	0.005	1e-7 - 1e0	s^{-1}
k_2	0.04	1e-7 - 1e0	$s^{-1}mm$
k_3	0.00004	1e-7 - 1e-1	s^{-1}

Data Analysis Methods

Trauma data was collected from 20 patients from one University of Pittsburgh clinical trial, the Study of Tranexamic Acid During Air Medial Prehospital transport trial (STAAMP). All TEG data were collected as a rapid TEG from Haemoscope's TEG 5000. Rapid TEGs were collected for each patient at approximately 0, 12, and 24 hours after enrollment in the clinical trial, re-

sulting in a total n=60 TEGs. Each TEG is composed of displacement measurements taken every five seconds for a total of approximately 4500 seconds. To map the raw measurement onto a traditional TEG displacement envelope, raw values from the device are divided by 4 and plotted twice: once as raw/4, and a second time reflected across the time axis. The model developed strictly simulates the positive portion of the TEG, since the bottom half is a simple reflection in the x-axis.

From the model structure described, parameter estimation and model solution were accomplished using a backward-difference formulation implementing the Interior Point OPTimizer, IPOPT solver (Wachter and Biegler, 2004). For this, the model was constructed in Python 3.5.1 using the PYthon Optimization Modeling Objects (PYOMO) 4.3 package (Hart et al., 2011, 2012) linked to IPOPT. Together the result minimizes the sum of squared error (objective function) between the data and the model at every time point. The resulting optimal values were recorded. The parameter bounds were found as stated in Table 1.

Markov Chain Monte Carlo Analysis

Parameter estimation, using the data from STAAMP, was accomplished using an Affine-Parallel Tempering Markov Chain Monte Carlo (APT-MCMC) algorithm (Zhang et al., 2015). For plotting parameter correlations for each data set, the last ten thousand sets of parameter vectors (of the one hundred thousand total) were extracted. The parameter distributions returned by APT-MCMC were further used to assess identifiability of parameters, possible interparameter correlations, and to establish the manifestation of disease endotypes.

APT-MCMC is a Markov Chain Monte Carlo (MCMC) algorithm. MCMC algorithms employ random walks along the objective function surface to search for minima. While less efficient than gradient-based solvers, MCMC algorithms are better able to search multi-modal surfaces where many minima exist. APT-MCMC uses the Metropolis-Hastings algorithm to locate, explore, and escape these minima. APT-MCMC also employs additional add-ons to improve search efficiency (Zhang et al., 2015). Parallel tempering, with information transfer between chains at different *temperatures*, employs an objective function surface scaling that facilitates breadth search (high temperatures that flatten the objective function surface) and depth search (lower temperatures exploring identified wells). Within each temperature is an ensemble of samplers with affine invariance (Goodman and Weare, 2010). This technique uses multiple walkers to explore the objective space with greater efficiency.

Results

The model in Eqs. (4)-(7) was fit to individual patients from the STAAMP trial. A simplified form of the model, using a linear dependence on Pa for thrombus formation rate, versus the quadratic dependence in (5), was also evaluated. On a test data set of 10 TEG tracings, a quantitative comparison between the two models showed the nonlinear model provided an 18.8 % decrease in sum-of-squared error (model prediction vs. data). As a result, it appears the quadratic dependence that yields a faster dynamic growth of the thrombus state, or rapid thrombus formation, is superior. Ultimately, this is consistent with robustness in biology – this process is responsible for stopping bleeding and is critical to organism survival.

Individual Patient Fits

When tested against the full data set (20 patients, 3 time points per patient), the model results in an average relative error of 6.42 percent (average SSE: 174 mm^2), quantifying the ability of the model to capture individual TEG data. An example TEG tracing set for a single patient over 3 time points is shown in Figure 1.

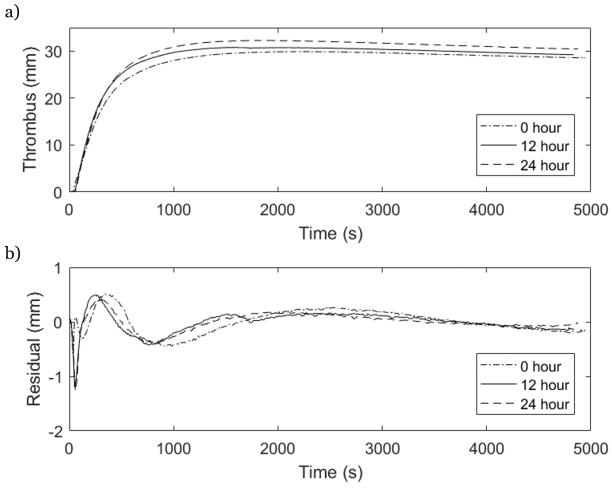

Figure 1. A representative set of TEG tracings for one STAAMP patient with (a) the raw data at all time-points, (b) the difference between the data and the model estimate.

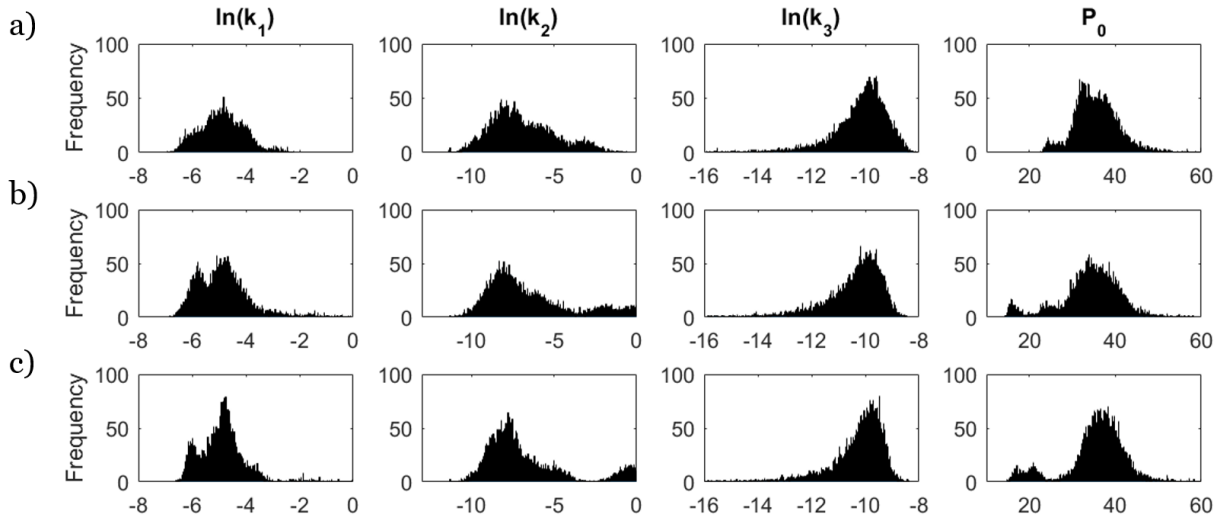

Figure 2. Parameter distributions from APT-MCMC model fits to TEG data for 20 patients at 0 hours (left), 12 hours (middle) and 24 hours (right). The last 10,000 parameter vectors from APT-MCMC fitting were used for each patient at each time point.

Figure 1(a) shows a typical set of patient TEG tracings at every time point. Thrombus forms quickly, leading to a peak in displacement amplitude between 1000 and 1500 seconds. Over time, the clot then breaks down via lysis, leading to a decrease in the displacement amplitude of the TEG. Figure 1(b) shows the residual error between the data and the fit of the model at each time point. For this patient, the model does not display an error at any time point of greater then approximately 1 mm. The model captures the data after the maximum amplitude is reached with minimal error. The residuals during the initial dynamic region is higher, suggesting a future improvement in model structure targeting platelet activation and thrombus growth.

Relating these fits to parameter values in the model is important for endotyping or identifying changes in patient coagulopathic state over time. The temporal trend in the TEGs in Figure 1(a) is that the maximum amplitude increases from the 0 hour to 12 hour to 24 hour time-points. This is generally captured by increases in the P_0 parameter over time. Additionally, the lysis rate is increasing slightly (via the larger difference between maximum and final values). The increase in k_3 captures this dynamic difference. Finally, the initial clotting dynamics, observed as the rising slope, increases in speed from 0 to 12 hours and then slightly increases again at the 24 hour time point. In the parameter estimation, this is quantified as k_1 increasing from 0 to 12 hours, and then staying the same between the 12 hour and 24 hour time-points. For this individual patient the model parameters for the three TEG fits at each time point are shown in Table 2.

Table 2. Parameter estimates for the representative patient at all three time-points.

Parameter	0 hours	12 hours	24 hours
P_0	30.7	32.0	33.9
k_1 (s^{-1})	0.0034	0.0046	0.0043
k_2 $(mm \times s^{-1})$	0.0055	0.0020	0.0016
k_3 (s^{-1})	1.38e-5	1.84e-5	2.21e-5

Population Fits using APT-MCMC

The model was fit to each data set using APT-MCMC. From the population analysis in Figure 2, the model parameters all appear identifiable from the clinical data.

Population histograms for all fits at each time point show easily identifiable maxima. Bimodalities appear in k_2 and P_0, particularly later in the time-course for both parameters. These latter results suggest the possible development of subpopulations. A separation in the population further supports the identification of patients that differ in their clinical prognosis or outcome, thereby motivating the study of patients based on their endotype, which could be identified in model parameter space.

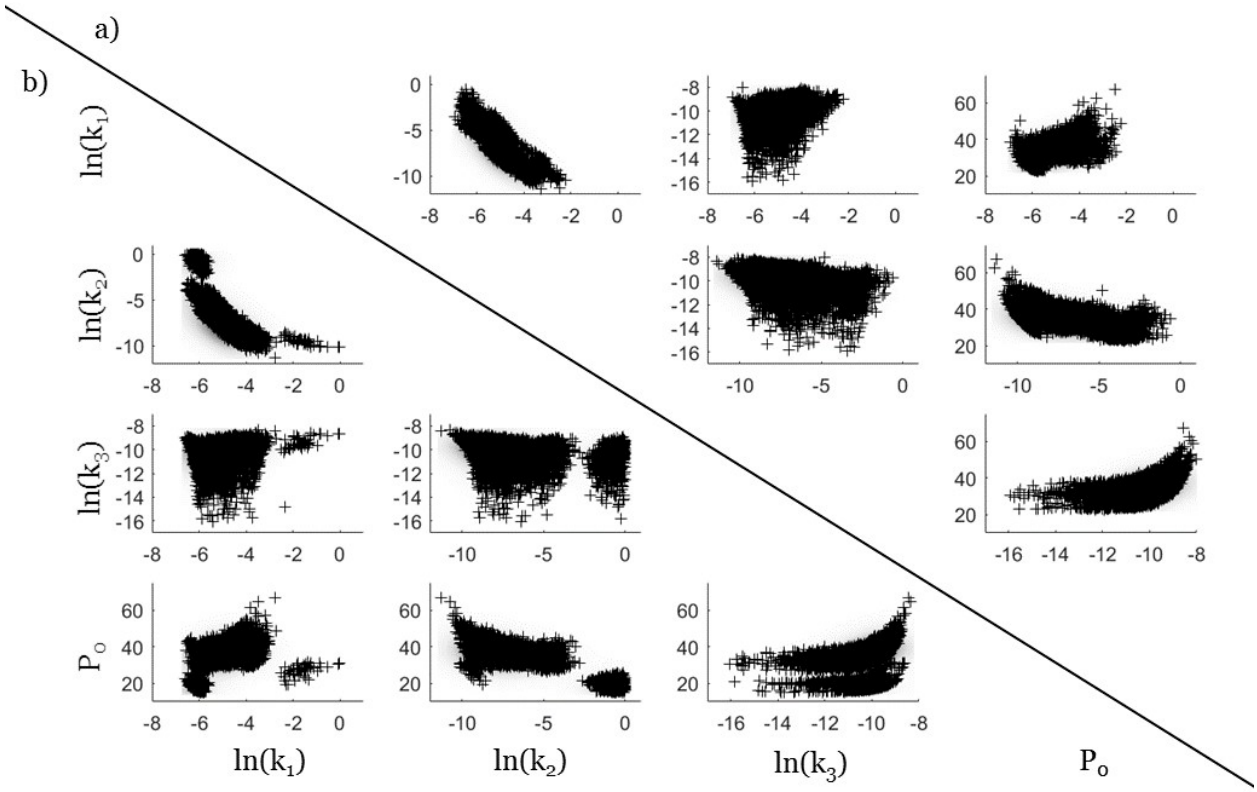

Figure 3. Parameter-parameter correlation plots from all model fits (last 10,000 parameter vectors per patient) at time = 0 hours (a) and time = 24 hours (b). Comparisons of interparameter correlations across time points can be made by reflecting across the diagonal of the figure. In (a), y-axis values are given by the row (in order downward, $\ln(k_1)$*,* $\ln(k_2)$*,* $\ln(k_3)$*, and* P_0*), x-axis is by column (same order as rows). Axes on the 24-hour plots (b) have been flipped (plots reflected in the unity line) to allow direct optical comparison with the time = 0 hours plots in (a).*

Interparameter Correlations

APT-MCMC facilitates the study of parameter correlations in a probabilisitic setting. Of particular interest is the ability to use apparent parameter correlations to either motivate model reduction/simplification by reducing the parameter space or to further establish endotypic differences that manifest in the parameter space. This analysis employs two-dimensional parameter plots (for each combination of parameters), as shown in Figure 3. A linear correlation between $\ln(k_1)$ and $\ln(k_2)$ is observed at the 0 hour time point, and the relationship between $\ln(k_2)$ and P_0 may also be linear at the 0 hour time point. At this same time point, a nonlinear correlation between $\ln(k_3)$ and P_0 is also evident. By the 24 hour time point, the $\ln(k_1)$ vs. $\ln(k_2)$ correlation has become multimodal in parameter space. The $\ln(k_3)$ vs. P_0 correlation remains, but has separated into two subpopulations, and the $\ln(k_2)$ vs. P_0 correlation has likewise been lost as a subpopulation arises. These subpopulations may indicate the manifestation of clinically-relevant endotypes within the population that can inform clinical outcome and may guide therapy. Upon completion of the STAAMP trial we will be able to discern whether we are observing temporal and interpatient changes that are established by therapeutic decision-making *a priori* (patients in STAAMP are randomized to receive, or not receive, tranexamic acid during transport), or as a result of treatment independent of the initial intervention (which would indicate potential endotypes within the population).

Conclusions

A low-order dynamic model of coagulation, as measured by TEG, was developed. The model is able to fit 20 individual patients across a clinical time-frame of 24 hours, by adjusting 3 rate parameters and a scaled version of the initial platelet count. Analysis via APT-MCMC indicates that parameters are identifiable from

TEG data, though nonlinear correlations between parameters may exist. Furthermore, when model fits are observed in parameter space, subpopulations manifest over time and interparameter correlations change. The effect of early interventions, and the emergence of endotypes within the population, will be evaluated as patient data are unblinded. Increases in model complexity, to better capture interpatient differences (*e.g.*, sex, race, body weight, trauma severity, other clinical measurables), are the topic of ongoing work.

Acknowledgments

Financial support for this work is provided by the Department of Education Graduate Assistance in Areas of National Need fellowship program (P200A120195, P200A150050). Partial support was provided by NIH/ NHLBI grant R21-HL-133891 An additional acknowledgment of help implementing the APT-MCMC algorithm needs to be made to Li Ang Zhang.

The authors declare no conflicts of interest.

References

(2007). *TEG 5000 Thromboelastograph Hemostasis System User Manual*. Haemoscope, teg analytical software (tas): version 4.2.3 edition.

Anand, M., Rajagopal, K., and Rajagopal, K. (2008). A model for the formation, growth, and lysis of clots in quiescent plasma. a comparison between the effects of antithrombin iii deficiency and protein c deficiency. *Journal of Theoretical Biology*, 253:725–738.

Bannish, B. (2014). Modelling fibrinolysis: a 3d stochastic multiscale model. *Mathematical Medicine and Biology*, 31:17–44.

Goodman, J. and Weare, J. (2010). Communications in applied mathematics and computational science: Ensemble samplers with affine invariance. *Comm. App. Math. and Comp. Sci.*, 5(1):65–80.

Hart, W. E., Laird, C., Watson, J.-P., and Woodruff, D. L. (2012). *Pyomo–optimization modeling in python*, volume 67. Springer Science & Business Media.

Hart, W. E., Watson, J.-P., and Woodruff, D. L. (2011). Pyomo: modeling and solving mathematical programs in python. *Mathematical Programming Computation*, 3(3):219–260.

Jones, K. and Mann, K. (1994). A model for the tissue factor pathway to thrombin. ii. a mathematical simulation. *Journal of Biological Chemistry*, 269(37):23367–23373.

Liou, D., Shafi, H., Bloom, M., Chung, R., Ley, E., Salim, A., Tcherniantchouk, O., and Margulies, D. (2014). Defining early trauma-induced coagulopathy using thromboelastography. *American College of Surgeons*, (10):994–998.

Lo, K., Denney, W., and Diamond, S. (2005). Stochastic modeling of blood coagulation initiation. *Pathophysiol Haemost Thromb*, 34:80–90.

Maegele, M., Lefering, R., Yucel, N., Tjardes, T., Rixen, D., Paffrath, T., Simanski, C., Neugebauer, E., and Bouillon, B. (2007). Early coagulopathy in multiple injury: An analysis from the german trauma registry on 8724 patients. *Injury, Int. J. Care Injured*, 38:298–304.

Maegele, M., Paffrath, T., and Bouillon, B. (2011). Acute traumatic coagulopathy in severe injuryincidence, risk stratification, and treatment options. *Dtsch Arztebl Int*, 108(49):827–835.

Wachter, A. and Biegler, L. (2004). On the implementation of an interior-point filter line-search algorithm for large-scale nonlinear programming.

Xu, Z., Lioi, J., Mu, J., Kamocka, M., Liu, X., Chen, D., Rosen, E., and Alber, M. (2010). A multiscale model of venous thrombus formation with surface-mediated control of blood coagulation cascade. *Biophysical Journal*, 98:1723–1732.

Zhang, L., Clermont, G., Banerjee, I., and Parker, R. (2015). Apt-mcmc: Parallel tempering markov chain monte carlo with affine-invariant ensemble samplers for parameter fitting. Presented at 2015 FOSBE conference, Boston, MA.